Involution symmetry quantification using recurrences

Gabriel Marghoti [1,2,*] Thiago de Lima Prado [1,3,4] Sergio Roberto Lopes,[1,3,5] and Yoshito Hirata [6]

[1] *Physics Department, Federal University of Paraná, Curitiba, Paraná 81530-015, Brazil*
[2] *Degree Program in Computer Science, University of Tsukuba, 1-1-1 Tennodai, Tsukuba, Ibaraki 305-8573, Japan*
[3] *Interdisciplinary Center for Science, Technology and Innovation CICTI, Federal University of Paraná, Curitiba 81530-015, Brazil*
[4] *Departament of Physics, University Rey Juan Carlos, Móstoles, 28933 Madrid, Spain*
[5] *Potsdam Institute for Climate Impact Research - Telegraphenberg, 14473 Potsdam, Germany*
[6] *Institute of Systems and Information Engineering, University of Tsukuba, 1-1-1 Tennodai, Tsukuba, Ibaraki 305-8573, Japan*

Symmetries are ubiquitous in science, aiding theoretical comprehension by discerning patterns in mathematical models and natural phenomena. This work introduces a method for assessing the extent of symmetry within a time series. We explore both microscopic and macroscopic features extracted from a recurrence plot. By analyzing the statistics of small recurrence matrices, our approach delves into microscale dynamics, facilitating the identification of symmetric time series segments through diagonal macroscale structures on a recurrence plot. We validate our approach by successfully quantifying involution symmetries for three-dimensional dynamical models, specifically, order-2 rotational symmetry in the Lorenz '63 model, and inversion symmetry in the Chua circuit. Our quantifier also detects symmetry breaking in the modified Lorenz model for *El Niño* phenomenon. The method can be applied in a versatile manner, not only to three-dimensional trajectories but also to univariate time series. Symmetry quantification in time series is promising for enhancing dynamical system modeling and profiling.

I. INTRODUCTION

Symmetry is a fundamental concept pervasive in every field of study, especially mathematics, physics, and biology [1–3]. It offers convenient frameworks for understanding various concepts and phenomena, and serves as a rigorous property that, when detected from data, can significantly enhance modeling efforts.

There is a noticeable gap in research concerning the impact of symmetric dynamical systems models in the time series analysis. This study addresses this gap, focusing on exploring time series from symmetric strange attractors, which exhibit flexible polarity reversals in specific system variables [4–8], facilitating coexisting attractors, alternative chaotic signals, the convenience of chaos application [9–11], and the design of complex dynamical systems modeling [12,13].

Recurrence plots [14,15] quantifiers are advanced time series analysis methods to extract information from nonlinear data. By assessing both microscopic and macroscopic structures derived from a recurrence plot, we utilize the set of generated recurrence motifs [16–18] in each particular row (or column) to better qualify the time series microstates at each time instant, which facilitates the detection of symmetry from time series.

To evaluate the effectiveness of our approach, we test it on two types of involution symmetries [19] for three-dimensional chaotic attractors. The first is the Lorenz '63 model [4], with rotation by π symmetry. The second is the Chua circuit

[20], which presents inversion symmetry for all its variables [19,21]. For the Lorenz model we also incorporate an additional symmetry-breaking parameter. This modification induces asymmetrical development in the attractor's wings, resembling the anomalous scenario observed in the *El Niño* climate pattern [22–25].

The paper is organized as follows: In Sec. II we introduce the background knowledge that is necessary to understand this paper, in Sec. III we develop the technique based on recurrences, and in Sec. IV we test the proposed quantifier. Then we discuss the results in Sec. V, and finally, in Sec. VI we summarize the article and provide suggestions for future work.

II. BACKGROUNDS

A. Symmetric dynamic models

In dynamic models the involution symmetry occurs when a time evolution rule remains unchanged under an involution transformation. The simplest type of such transformation is represented by the function $f(x) = -x$, which is its inverse so $f(f(x)) = x$ [19]. For three-dimensional chaotic systems, the symmetry is classified as reflection, rotation (by π), or inversion, depending on which variables adhere to this transformation [21].

To evaluate rotation by π symmetry, we propose the analysis of the Lorenz '63 model [4], which can be written as

$$\dot{x} = -s(x - y),$$
$$\dot{y} = -xz + gx - y, \qquad (1)$$
$$\dot{z} = xy - bz,$$

*Contact author: gabrielmarghoti@gmail.com

where we use the typical values $s = 10$, $g = 28$, and $b = 8/3$, which generate a chaotic attractor. This model exhibits symmetry, as its dynamic equations remain unchanged under the transformation $x \to -x$, $y \to -y$, and $z \to z$ [26].

The inversion symmetry occurs when the equations of motion are equivalent under the transformation $(x, y, z) \to (-x, -y, -z)$. A model that has such a property is the Chua circuit [20], here used in its simplified version,

$$
\begin{aligned}
\dot{x} &= a(y - x - g(x)), \\
\dot{y} &= x - y + z, \\
\dot{z} &= -by,
\end{aligned}
\tag{2}
$$

where the variables represent the voltages across two capacitors and the current of the inductor, respectively; a and b are parameters related to resistance, capacitance, and inductance. The function $g(x)$ is piecewise linear, representing a non-Ohmic resistor,

$$
g(x) = m_1 x + \frac{(m_0 - m_1)}{2}(|x + 1| - |x - 1|), \tag{3}
$$

where m_0 and m_1 are the slopes associated with the change in resistance, the only nonlinear component in the circuit. The function $g(x)$ can be defined differently without losing the qualitative dynamics; however, it needs to be an odd function for the system to be equivalent under the inversion transformation. To generate a chaotic double-scroll attractor, we set the parameters $\alpha = 15.6$, $\beta = 28.0$, $m_0 = -8/7$, and $m_1 = -5/7$.

Let us write a set of differential equations concisely as $\dot{x} = f(x)$. In a time series from the symmetric nonlinear system, the distance between two vectors remains unchanged after a symmetry transformation. Consider a time series vector x_i and its respective symmetric vector $s_i = I(x_i)$, given by an involution symmetry, specifically an inversion or a rotation by π transformation such that we also have $\dot{s} = f(s)$ with the resulting symmetric variables s.

Each variable can be transformed either through the identity $I_j(x) = x_j$ or its sign reversal $I_j(x) = -x_j$. In both cases, the absolute value is preserved. This transformation is associative and follows the property $x_i = I(s_i)$.

In this context, the distances respect the relation

$$
\|x_i - x_j\| = \|I(s_i) - I(s_j)\| = \|I(s_i - s_j)\| = \|s_i - s_j\|, \tag{4}
$$

where $\|\cdot\|$ denotes the norm (e.g., Euclidean).

Therefore, if the trajectory presents vectors such that $x_k = s_i$ and $x_p = s_j$, each trajectory instant has the same distance statistics as an instant in its symmetric state. In practice, this property only holds for a periodic time series; in a chaotic attractor, the trajectory can only recur to a small neighborhood of a specific state in finite time so $x_k \approx s_i$ and $x_p \approx s_j$. Consequently, the distribution of distances around symmetric coordinate points in chaotic systems should be alike. This property is hypothesized to generate similar rows or columns for symmetric instants in a recurrence plot, which we exploit and test using our proposed quantifier.

B. Asymmetric Lorenz '63 model

To analyze the loss of symmetry, we add an asymmetry constant to the original Lorenz model variable x. The modified model is based on the Vallis system, which is the Lorenz system with a parameter breaking the rotation symmetry. It is one of the simplest chaotic models for the *El Niño* anomaly [22,24]. It is mathematically expressed by

$$
\begin{aligned}
\dot{x} &= -s(x - y) + \varepsilon, \\
\dot{y} &= -xz + gx - y, \\
\dot{z} &= xy - bz,
\end{aligned}
\tag{5}
$$

where we set $s = 10$, $g = 28$, $b = 8/3$, and ε is the symmetry-breaking parameter. Notice this only has rotation symmetry if $\varepsilon = 0$.

In Fig. 1 we plot two trajectories of the modified Lorenz model, one unperturbed and the other with a high-asymmetry parameter value. For the plots and analysis, we used a sampling step size of 0.1, a time series of size $N = 5000$ collected after an equal-size transient, and integrated with 0.01 time step using the fourth-order Runge-Kutta method.

The asymmetric model shows a tendency for trajectories to remain longer in the positive x-value wing. Both wings are preserved, but the vector field is not symmetric so one wing is not the symmetric of the other. Our method aims to quantitatively detect this symmetry breaking by analyzing the recurrence statistics of trajectory points, with no prior knowledge of the attractor structure.

C. Recurrence plots

Recurrence plots (RPs) were first proposed by Eckmann *et al.* [14] in 1987 and have been improved since then [15,27]. Nowadays, it is a significant technique in time series analysis, and studies propose that the plot encapsulates all essential dynamical information [28,29]. Yet, there is still undeveloped potential in exploring recurrences [15].

A recurrence plot is a binary matrix. Mathematically, an RP can be written as

$$
R_{ij} = \Theta(\epsilon - \|x_i - x_j\|), \tag{6}
$$

where $\Theta(\cdot)$ is the Heaviside function and ϵ is the recurrence threshold. The trajectory $\{x_t\}$ is evaluated in distinct time frames i and j. This work uses the Euclidean distance to assess the proximity between trajectory points.

The conventional quantifiers derived from recurrence plots usually involve examining specific patterns within the plot, such as the (non)recurrent diagonal or vertical lines [15]. Recent research has focused on evaluating generic small matrices (motifs) derived from RPs to characterize both stochastic and deterministic properties of time series [16]. The diversity observed within these motifs facilitates entropy measurement [16], parameter-free quantification of stochastic and chaotic signals [17]. Moreover, it also contributes to the characterization of random dynamical systems [18].

In this context, our approach broadens as we gather information from all possible patterns of a designated size, referred to as recurrence motifs (RM), which are small matrices within an RP, defined by $RM(i, j, k, L) = \{R_{ab} \mid a = i, i + 1, \ldots, i + L - 1; b = j, j + 1, \ldots, j + L - 1\}$, where L is
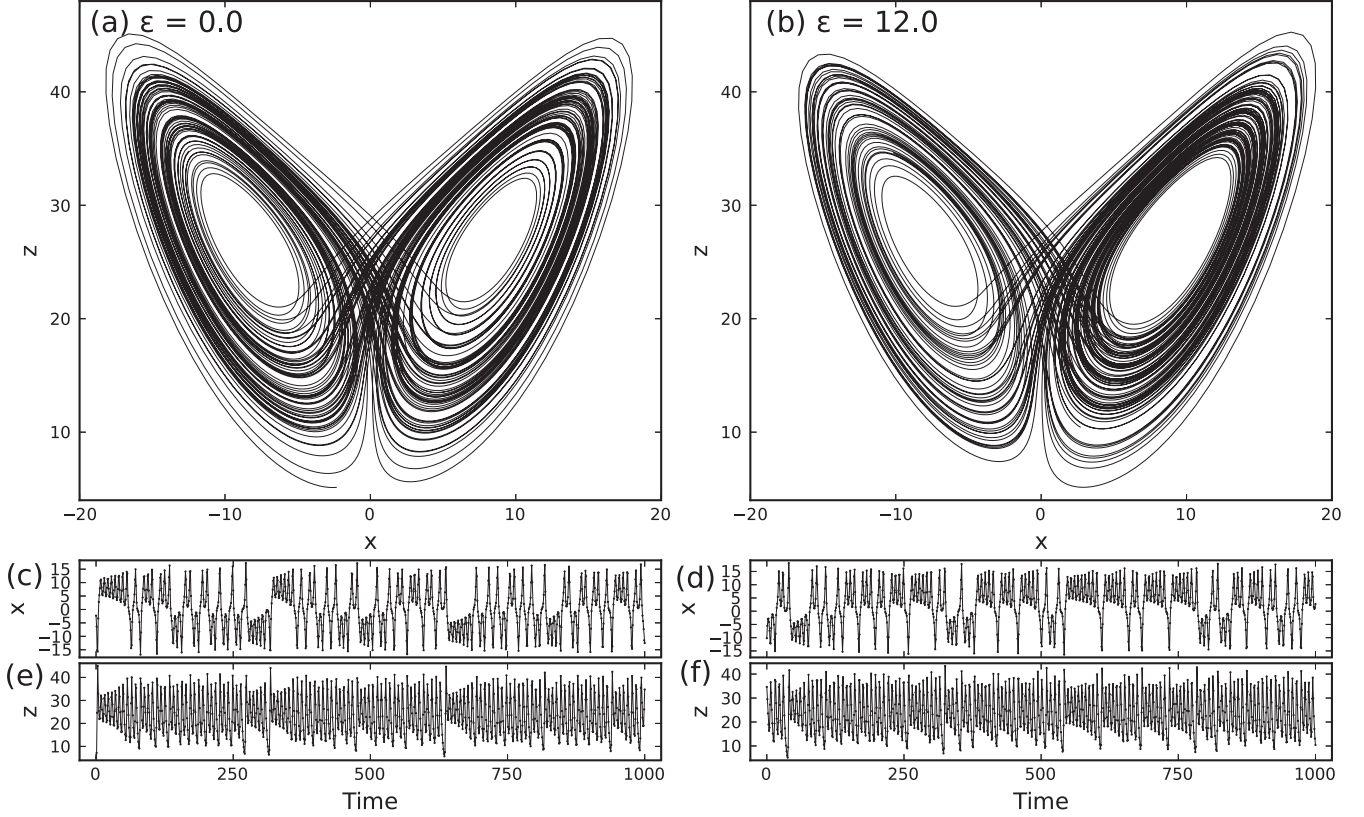
FIG. 1. Modified Lorenz '63 model dynamics, left panels illustrate the symmetric case while the right panels depict asymmetric dynamics. The trajectory on the x-z plane for (a) the original symmetric model and (b) for the asymmetric model with parameter $\varepsilon = 12.0$. The bottom panels display the time series for (c) and (d) component x, and (e) and (f) component z.

the motif size and $k = 1, \ldots, 2^{L^2}$ is the motif index encompassing all the possible recurrence configurations for a square matrix of side L.

III. THE PROPOSED METHOD

For a symmetry quantification of time series, we need a better qualification of data points than their measured values. In this sense, here we introduce a time series representation as a sequence of pattern probabilities associated with each time instant, named, recurrence motif probability distributions. In contrast to other variations that rely on the recurrence of distinct features beyond the phase space distance, such as isodirectional segments [30], ordinal pattern symbolic dynamics [31], or representing time series as a time-ordered sequence of probability density functions [32], our proposed recurrence plot variation maintains its foundation in structures derived from the usual RPs. In Fig. 2 we present an overview of the method, which described next.

A. Microstate description of a time series

The microstate consists of values that more accurately describe the dynamics at each moment. We start with the RP of a time series $\{x_t \mid t = 1, 2, \ldots, N\}$ given by the matrix R_{ij}. In this framework the recurrence patterns generated each time correspond to a specific row (or column) on the RP. Therefore

to define the microstate based on recurrences of our time series, we use the recurrence motifs concept [16–18].

Next, we systematically gather square motifs from the RP at each fixed time index, ensuring that each time instant is associated with a probability distribution of recurrence motifs. We convert the time series in a sequence of probability distribution $\{\boldsymbol{P}_t \mid t = 1, 2, \ldots, N - L + 1\}$, with each component k given by $[\boldsymbol{P}_t]_k = \Pr[RM(t, t', k, L) \mid t' = 1, 2, \ldots, N - L + 1]$, which we use as the microstate description of a time series.

This represents constructing a histogram for each row from the recurrence plot, encompassing all potential 2^{L^2} motifs, and subsequently normalizing by the total number of collected elements within the row of width L starting at time t. In this way the $\boldsymbol{x}_t$ values associated with consecutive microstates overlap. For instance, $\boldsymbol{P}_t$ is associated with segment $\boldsymbol{x}_t, \boldsymbol{x}_{t+1}, \ldots \boldsymbol{x}_{t+L-1}$ and $\boldsymbol{P}_{t+1}$ is associated with segment $\boldsymbol{x}_{t+1}, \boldsymbol{x}_{t+2}, \ldots \boldsymbol{x}_{t+L}$.

The RP for the probabilities time series $\{\boldsymbol{P}_t \mid t = 1, 2, \ldots, N - L + 1\}$ defines the motif probability distribution recurrence plot (PR) as

$$\mathrm{PR}_{ij} = \Theta(\epsilon_{\mathrm{PR}} - d(\boldsymbol{P}_i, \boldsymbol{P}_j)), \tag{7}$$

where ϵ_{PR} is the threshold to ascertain if two times generate a similar motif distribution on their RP rows. For the PR_{ij} matrix computation we use the Hellinger distance [33], which is appropriate for probability distribution comparison.
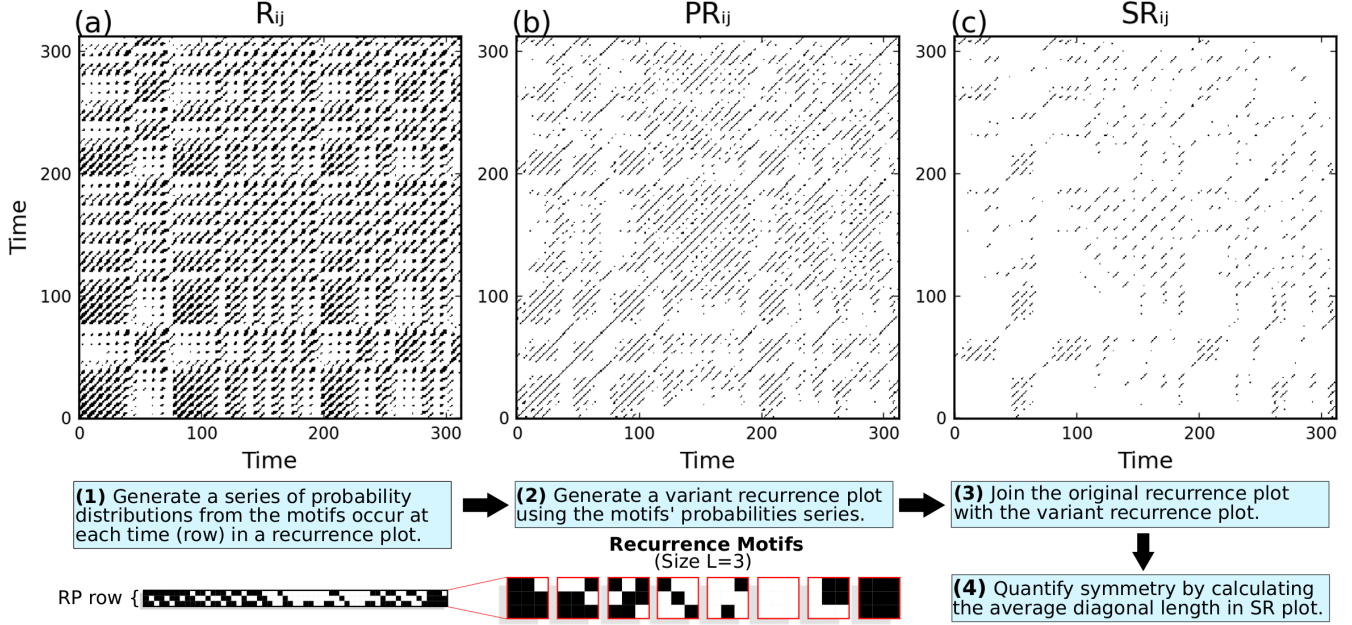
FIG. 2. Method based on recurrence to identify symmetry on a time series. In all plots, black regions correspond to a matrix value of 1, while white corresponds to a value of 0. In panel (a) the original recurrence plot for the Lorenz '63 model is presented; in (b) the recurrence plot utilizes the probability distribution of motifs series, with one probability distribution for each row from the original plot; and in (c), the symmetry recurrence plot is demonstrated, representing the joint product between the first two matrices, that is, PR_{ij} and $(1 - R_{ij})$. For this example we used the three-dimensional Lorenz '63 system, which has symmetry for variables x and y, a 20% recurrence rate for R_{ij}, motifs' size $L = 3$, and $\epsilon_{PD} = 0.2$ for the PR_{ij} construction. The bottom panels represent the method diagram in four steps to set up the symmetry quantifier and some examples of typical motifs collected within an RP row.

B. Symmetry quantification

Recurrences in PR encompass any time pair with a similar row structure on the RP regardless of their proximity, more rigorous time instants that satisfy Eq. (4). Therefore, to detect similar dynamics only at distant trajectory points, we have to filter trivial recurrences due to the proximity in the phase space. To solve this we combine the times with similar motif probability $PR_{ij} = 1$ and the times with no recurrence, $R_{ij} = 0$.

The joint recurrence plot [34] between PR_{ij} and $(1 - R_{ij})$, which we refer to as a symmetry recurrence plot (SR), is defined as

$$SR_{ij} = PR_{ij}(1 - R_{ij}), \qquad (8)$$

where the value 1 in this plot indicates a pair of times i and j with similar microstate dynamics but distant in the state space. The SR matrix size matches PR because we do not use the last $(L - 1)$ points' part of the time series for R_{ij} to form the Hadamard product.

Additionally, we will show that the count of recurring points in SR_{ij} may not precisely measure the symmetry of chaotic attractors. For a more accurate measurement of symmetry, it is necessary that two distant trajectory segments consistently present a similar microstate sequence.

Similarly to the well-known quantifier of determinism from RPs [15], the diagonal lines parallel to the main diagonal denote similar dynamics segments, but in the SR plot such sequences are related to reflected time sequences. Consequently, here we propose a quantifier for the estimation of symmetry

based on the diagonal line length,

$$SYM = \frac{\sum_{l=l_{\min}}^{N-L+1} lP(l)}{\sum_{l=1}^{N} lP(l)}, \qquad (9)$$

where $P(l)$ is the probability of finding a diagonal line with length l in the SR_{ij} matrix, and $l_{\min}$ is the minimal line length of consecutive diagonal line segments on SR that contributes to the numerator of the index SYM [Eq. (9)]. Although the optimal parameters to improve the efficacy of quantifiers based on diagonal line lengths remain an open question [35], in this work we choose the generally used value $l_{\min} = 2$. In this way, SYM is a recurrence-based quantifier restricted to a range between 0 and 1. The higher its value, the more symmetric the time series is.

Our approach is designed for the comparative analysis of diverse time series, and it relies on a sufficiently detailed R_{ij} matrix. For consistency, employing a fixed recurrence rate for the R_{ij} matrix may be advised to be used, ensuring that various RPs have an equal opportunity to generate patterns, at least concerning the number of recurrences. In this context, employing a defined threshold ϵ_{PR} for PR_{ij} yields robust results, as we will demonstrate in the following section.

C. Qualitative example

To provide a qualitative understanding of the method's operation, as a visual tool to assess dynamics information from the observed trajectory, Fig. 2 displays example plots of the three proposed matrices for symmetry estimation, employing the symmetric Lorenz model [Eq. (1)]. Panel (a) depicts
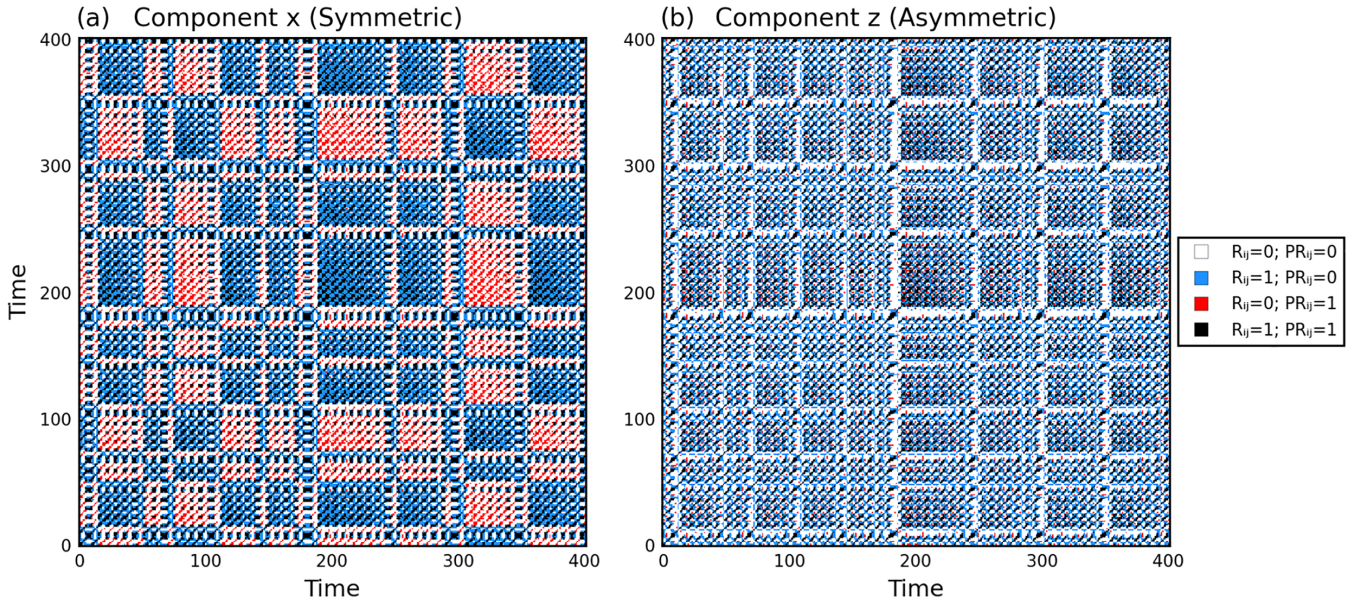
FIG. 3. Joint plot for the recurrences of time series values (R_{ij}) and the motifs probabilities values (PR_{ij}) for components (a) x and (b) z of the Lorenz '63 model. The parameters for the plots are a fixed recurrence rate value $RR = 0.5$ for R_{ij} matrix, a fixed threshold of $\epsilon_{PR} = 0.3$, and motif size $L = 2$ for PR_{ij}. The panels depict distinct structures in the joint recurrence plot from (a) symmetric and (b) asymmetric time series. White regions denote the absence of recurrence for both time series values and motif probability distribution space. Blue signifies recurrences solely of time series values. Red regions represent no recurrence in the time series space but recurrence in the motif probability distribution space, serving as an indicator for symmetry. Black color corresponds to times with similar values and similar motif distribution.

the typical recurrence plot, while panel (b) illustrates the recurrence of motif probability distributions PR_{ij}, and panel (c) presents the joint plot SR_{ij}, which highlights symmetric patterns within a time series.

The PR_{ij} matrix tends to form diagonal structures, indicating the time evolution of microstates is coherent over distinct trajectory instants, generating fewer artifacts than the standard RP. So this RP variation differs from R_{ij} because its main benefit is the capability to detect time sequences with similar dynamics evolution regardless of their position on the phase space.

On the other hand, the SR_{ij} matrix exhibits shorter diagonal lines and more isolated points compared to PR_{ij}. Trajectories at symmetrically distant coordinates evolve according to the same rules over time, but the system may not recur exactly to the symmetry location due to the chaotic nature of the dynamics. Therefore, the lengths of diagonal lines in the SR_{ij} plot indicate how long trajectories tend to recur to *almost* symmetric segments. In practice, the longer the analyzed trajectory, the more likely it is to observe closer recurrences to symmetric locations in phase space.

Certain factors may hinder the correct match between trajectory points at a coordinate and their respective symmetric counterpart. Such factors could impede the observation of long symmetric segments or foster false symmetric segment measurements. We list contributions from asymmetric components, regions characterized by large Lyapunov exponents, and inadequate motif statistics (stemming from a short dataset or inappropriate recurrence threshold).

IV. RESULTS

To test our method on examples, we compare the performance between symmetric and asymmetric time series and present the recurrence matrices in the same diagram. Figure 3 presents the recurrence plot (R_{ij}) and the motif probability distribution plot (PR_{ij}) for components x and z from the symmetric Lorenz '63 model, where the intersections of $R_{ij} = 0$ and $PR_{ij} = 1$ correspond to $SR_{ij} = 1$, or $SR_{ij} = 0$ otherwise.

The recurrence plots of the components x and z have been constructed with the same recurrence rate, which ensures the same possibility of variability on the motifs within the RP. The compound RP and PR plots reveal additional structures in regions with and without recurrences in the phase space that correspond to $R_{ij} = 0$ with $PR_{ij} = 1$ and $R_{ij} = 1$ with $PR_{ij} = 0$.

The presence of structured patterns, where $PR_{ij} = 1$ and $R_{ij} = 0$, signifies the detection of dynamic properties within an RP region where no information was anticipated by conventional analysis. This phenomenon is more pronounced in the symmetric component plot [Fig. 3(a)], attributed to the inherent property of these structures to share identical dynamic equations across distant points in the phase space.

Although the asymmetric component also exhibits instances of $SR_{ij} = 1$, it is presumed that these points are incidental occurrences, because they do not form diagonal structures. Consequently, for the asymmetric component, each trajectory point mostly shares a similar motif distribution with its neighbors.

Our approach is suitable for analyzing dynamics in single-component time series, as it filters potential artifacts from trajectory projection onto a single component, and the SYM quantifier exclusively considers diagonal structures within the SR_{ij} plot. Prior studies suggest that recurrence-based statistics relying on diagonal structures parallel to the main diagonal demonstrate comparable performance, whether the phase space is reconstructed or not [36,37].

In addition, we believe the analysis of PR_{ij} and R_{ij} reveals information about artifacts, which are undesirable recurrences generated from false neighbors (e.g., when using just one variable to construct the RP) or orthogonal motion for recurring instants (expected to happen for high recurrence threshold values) [30]. The condition $R_{ij} = 1$ with $PR_{ij} = 0$ indicates that a recurrence using the time series does not match a recurrence in the microstates description, suggesting artifact recurrences. This result implies that our method estimates not only time series instants with symmetric properties but also similar values that do not correspond to the same phase space state.

To ascertain the parameter range within which our method operates effectively, Fig. 4 illustrates the dependency of SYM [Eq. (9)] on the recurrence plots parameter, more specifically, the recurrence rate and the recurrence threshold. We show the range for which the quantifier has consistent results and that motifs of size $L = 1$ cannot distinguish symmetric and asymmetric variables properly. Curve disruptions are caused by plots SR with no symmetric time series instants, a condition that makes the SYM value undefined, indicating an extreme degree of asymmetry in the time series or insufficient motif variety on the recurrence plot.

There are better recurrence parameter values that optimize the method. The most relevant one is the recurrence rate for the R_{ij} plot, ensuring diverse motifs are generated to capture system dynamics accurately. Limitations arise at both low and high recurrence rates. Low rates result in an overflow of non-recurring motifs. Conversely, high rates saturate the number of fully recurring motifs, diminishing variety and hindering accurate representations of system dynamics.

Comparing the performance on the Lorenz '63 symmetric variable x and asymmetric variable z, we find the threshold range ϵ_{PR} for distinguishing symmetry within time series is typically between 2×10^{-2} and 2×10^{-1}. High ϵ_{PR} treats all RP rows similarly and inflates the diagonal line count for SYM due to a lack of discrimination. Low value constraints are due to the time series size, as precision in $\{\boldsymbol{P}_t\}$ components depends on the number of elements in each RP row.

The Chua circuit SYM quantification indicates a high degree of symmetry for the same range as the Lorenz '63 model. As expected, both x and z components present symmetry with similar values for all the motif sizes considered. In this case, even motifs of size 1 were enough to detect symmetry, indicating that no influence of asymmetric variables on the analyzed time series facilitates symmetry detection for a system with inversion symmetry.

To extend the test on the capabilities of the SYM quantifier, we analyze the modified Lorenz '63 model changing the symmetry-breaking parameter. In Fig. 5 we show the symmetry quantification for the three-component trajectory and each component, considering size 2 or 3 motifs.
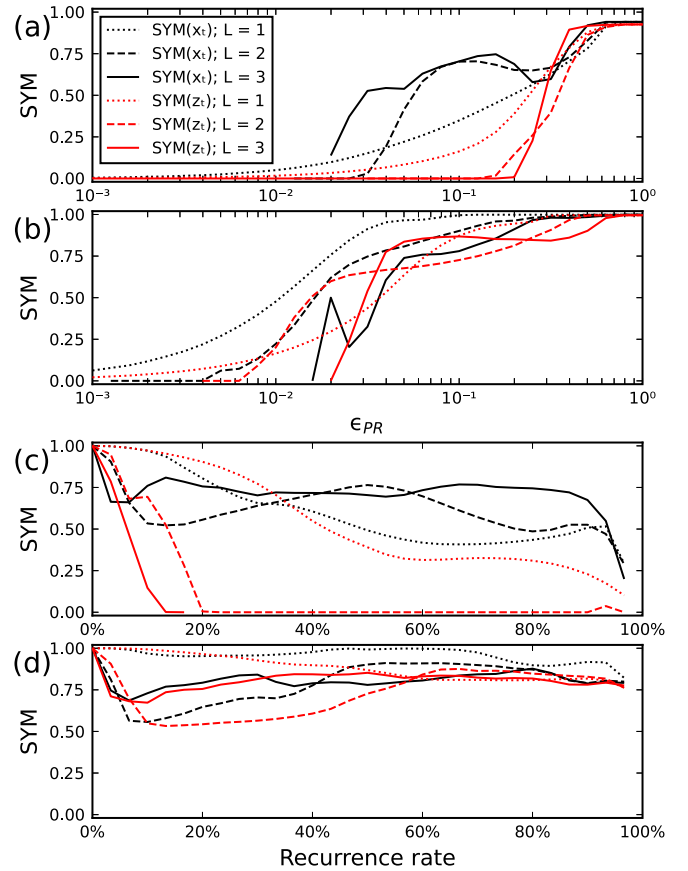

FIG. 4. Symmetry quantifier dependence on recurrence plot parameters for the Lorenz '63 models in panels (a) and (c), and Chua circuit in panels (b) and (d). In panels (a) and (b) we consider the SYM [Eq. (9)] as a function of the ϵ_{PR} threshold while maintaining a fixed 50% recurrence rate. In panels (c) and (d) we consider the dependence on the recurrence rate for a fixed $\epsilon_{PR} = 0.1$ threshold. We compare the performance of our quantifier for each variable and certain motif sizes L.
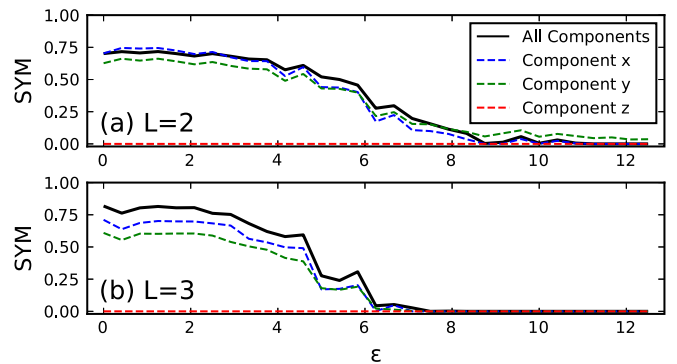

FIG. 5. Symmetry-breaking quantification on the modified Lorenz '63 model, considering a recurrence rate of 50% for the R_{ij} matrix and $\epsilon_{PR} = 0.1$ for the PR_{ij} matrix. Panel (a) presents the results for motifs of size $L = 2$, while panel (b) shows the results for size $L = 3$ motifs. We test for all components in solid black, component x in dashed blue, component y in dash-dot green, and component z in dotted red.

The components x and y, along with the entire trajectory, exhibit symmetry when $\varepsilon = 0$. Our approach effectively discerns the impact of the symmetry-breaking parameter. Despite introducing an asymmetry term to variable x, the time series of variable y and the three-dimensional trajectory similarly lose symmetry. This highlights our capability to detect the indirect effects of asymmetry terms.

In contrast, component z lacks symmetry, even in the original Lorenz '63 model. Consequently, the influence of the asymmetric parameter ε does not impact the symmetry (SYM) value for this component. Size-2 motifs still capture some symmetric trajectory points satisfying Eq. (8), which are not detected as symmetric segments, so the SYM value for the asymmetric component remains near zero.

On the other hand, the size-3 motifs have a more pronounced measure of symmetry breaking, having a higher contrast between symmetric and asymmetric time series. They detect differences among variables as ε increases and reaches SYM = 0.0 before the case using the size-2 motif.

V. DISCUSSIONS

All tests conducted indicate that larger motifs provide a better quantification of symmetry. The most significant improvement is observed when moving from motif size 1 to size 2, suggesting that motifs of size $L = 2$ are sufficient for accurately quantifying symmetry in the Lorenz '63 system. However, larger motifs can detect symmetry breaking for lower values of symmetry-breaking parameters.

The motifs of size larger than 1 quantify more than the distance distribution for each trajectory instant. They also consider how the distances of consecutive times relate to other values in the time series. Motifs with a size of 1 cannot properly detect symmetry, likely because their probability distribution captures only the local recurrence rate information.

For larger motifs, we get a better measure of symmetry. Therefore understanding symmetry requires more than just knowing the probability of individual points repeating. So, the probability distribution of motifs from the recurrence plot is good at capturing dynamic information for each time in a time series because they trace the relations between segments of data rather than isolated value distances.

In this work we chose to vary the recurrence thresholds and recurrence rates for RPs. Still, previous works on the recurrence motifs have proposed an entropy maximization principle to assert the optimal values [16,17]. Such a principle might provide a parameterless improvement of our method in a way that promotes diversity of motifs, which should improve the microstates profiling to create the PR matrix.

The method described in this context is not suitable for measuring symmetric states near the origin, particularly as seen in the Lorenz model, in cases where the trajectory changes wings. However, we anticipate that this limitation does not significantly impact the symmetry estimation of an attractor because it typically affects only a small portion of trajectory points.

Currently, we use the square motifs of size 2 or 3 in a recurrence plot to obtain the motif probability for each row. We could estimate the motif probability for each row appropriately here with $L = 3$, because the size of a recurrence plot is about 5000, even though the variety 2^{L^2} of the possible square motifs makes 512. In the future we may have to use the recurrence triangles [18] to construct the motif probability, because a recurrence plot is symmetric to the central diagonal line, and the number of possible kinds of recurrence triangles is reduced to $2^{\frac{L(L-1)}{2}}$.

VI. CONCLUSIONS

Understanding dynamical systems is crucial for advancing data assimilation and modeling. We introduce a method for quantifying inherent symmetry in time series using microscopic and macroscopic features of recurrence plots. Our method applies to order-2 rotation symmetry and inversion symmetry, and it detects the symmetry of individual variables or the entire trajectory.

By analyzing the influence of symmetry on the probability distribution of motifs in recurrence plots, we deduce the symmetry level in underlying dynamics. Symmetric systems show consistent dynamics across time segments, while asymmetric systems exhibit similarities only at recurring instants. Our method effectively detects symmetry on the Lorenz '63 model and the Chua circuit, just as the asymmetry introduced in the Lorenz attractor by a symmetry-breaking parameter.

Future work will extend this method to a broader range of deterministic and stochastic systems, test experimental data, and refine empirical models based on observed symmetry. Potential improvements include phase space reconstruction, alternative distance metrics, and optimizing motif statistics through recurrence entropy maximization [38].

Our findings demonstrate that recurrence motifs effectively characterize local dynamics (microstate) from a time series, highlighting the need for further research into symbolic dynamics approaches based on recurrences [39]. We are confident that our method will significantly advance the analysis and modeling of complex dynamical systems.

[1] H. Weyl, *Symmetry* (Princeton University Press, Princeton, NJ, 2015), Vol. 104.

[2] M. Tinkham, *Group Theory and Quantum Mechanics* (Courier Corporation, North Chelmsford, MA, 2003).

[3] E. Noether, Invariante variations probleme, Transp. Theory Stat. Phys. **1**, 186 (1971)..

[4] E. N. Lorenz, Deterministic nonperiodic flow, J. Atmos. Sci. **20**, 130 (1963).

[5] L. Chua, M. Komuro, and T. Matsumoto, The double scroll family, IEEE Trans. Circuits Syst. **33**, 1072 (1986).

[6] G. Chen and T. Ueta, Yet another chaotic attractor, Int. J. Bifurc. Chaos Appl. Sci. Eng. **09**, 1465 (1999).

[7] W. F. Langford, Numerical studies of torus bifurcations, in *Numerical Methods for Bifurcation Problems: Proceedings of the Conference at the University of Dortmund 1983* (Springer, 1983), pp. 285–295.

[8] A. L. Shil'nikov, On bifurcations of the Lorenz attractor in the Shimizu-Morioka model, Phys. Lett. A **62**, 338 (1993).

[9] C. Li, Z. Li, Y. Jiang, T. Lei, and X. Wang, Symmetric strange attractors: A review of symmetry and conditional symmetry, Symmetry **15**(8), 1564 (2023).

[10] B. A. Boya, B. Frederick, A. A. Danao, L. K. Kengne, and J. Kengne, Control and symmetry breaking aspects of a geomagnetic field inversion model, Chaos **33**, 013139 (2023).

[11] Y. Hirata and K. Aihara, Deep learning for nonlinear time series: Examples for inferring slow driving forces, Int. J. Bifurcation Chaos **30**, 2050226 (2020).

[12] Y. Guan, S. L. Brunton, and I. Novosselov, Sparse nonlinear models of chaotic electroconvection, R. Soc. Open Sci. **8**, 202367 (2021).

[13] W. A. Barbosa, A. Griffith, G. E. Rowlands, L. C. Govia, G. J. Ribeill, M.-H. Nguyen, T. A. Ohki, and D. J. Gauthier, Symmetry-aware reservoir computing, Phys. Rev. E **104**, 045307 (2021).

[14] J.-P. Eckmann, S. Kamphorst, and D. Ruelle, Recurrence plots of dynamical systems, Europhys. Lett. **4**, 973 (1987).

[15] N. Marwan, M. C. Romano, M. Thiel, and J. Kurths, Recurrence plots for the analysis of complex systems, Phys. Rep. **438**, 237 (2007).

[16] G. Corso, T. d. L. Prado, G. Z. d. S. Lima, J. Kurths, and S. R. Lopes, Quantifying entropy using recurrence matrix microstates, Chaos **28**, 083108 (2018).

[17] S. R. Lopes, T. L. Prado, G. Corso, G. d. S. Lima, and J. Kurths, Parameter-free quantification of stochastic and chaotic signals, Chaos Solit. Fractals **133**, 109616 (2020).

[18] Y. Hirata, Recurrence plots for characterizing random dynamical systems, Commun. Nonlinear Sci. Numer. Simul. **94**, 105552 (2021).

[19] J. C. Sprott, Simplest chaotic flows with involutional symmetries, Int. J. Bifurc. Chaos Appl. Sci. Eng. **24**, 1450009 (2014).

[20] T. Matsumoto, A chaotic attractor from Chua's circuit, IEEE Trans. Circuit Syst. **31**, 1055 (1984).

[21] C. Letellier and R. Gilmore, Covering dynamical systems: Twofold covers, Phys. Rev. E **63**, 016206 (2000).

[22] G. K. Vallis, El Niño: A chaotic dynamical system? Science **232**, 243 (1986).

[23] B. M. Garay and B. Indig, Chaos in Vallis' asymmetric Lorenz model for *El Niño*, Chaos Solit. Fractals **75**, 253 (2015).

[24] M. Borghezan and P. C. Rech, Chaos and periodicity in Vallis model for El Niño, Chaos Solit. Fractals **97**, 15 (2017).

[25] D. Alexandrov, I. Bashkirtseva, and L. Ryashko, Noise-induced chaos in non-linear dynamics of El Niños, Phys. Lett. A **382**, 2922 (2018).

[26] C. Letellier, P. Dutertre, and G. Gouesbet, Characterization of the Lorenz system, taking into account the equivariance of the vector field, Phys. Rev. E **49**, 3492 (1994).

[27] N. Marwan and K. H. Kraemer, Trends in recurrence analysis of dynamical systems, Eur. Phys. J. Spec. Top. **232**, 5 (2023).

[28] M. Thiel, M. C. Romano, and J. Kurths, How much information is contained in a recurrence plot? Phys. Lett. A **330**, 343 (2004).

[29] Y. Hirata, S. Horai, and K. Aihara, Reproduction of distance matrices and original time series from recurrence plots and their applications, Eur. Phys. J. Spec. Top. **164**, 13 (2008).

[30] S. Horai, T. Yamada, and K. Aihara, Determinism analysis with iso-directional recurrence plots, IEEJ Trans. Electron. Inf. Syst. **122**, 141 (2002).

[31] A. Groth, Visualization of coupling in time series by order recurrence plots, Phys. Rev. E **72**, 046220 (2005).

[32] B. Goswami, N. Boers, A. Rheinwalt, N. Marwan, J. Heitzig, S. F. Breitenbach, and J. Kurths, Abrupt transitions in time series with uncertainties, Nat. Commun. **9**, 48 (2018).

[33] E. Hellinger, Neue begründung der theorie quadratischer formen von unendlichvielen veränderlichen, Journal für die reine und angewandte Mathematik **1909**, 210 (1909).

[34] M. C. Romano, M. Thiel, J. Kurths, and W. von Bloh, Multivariate recurrence plots, Phys. Lett. A **330**, 214 (2004).

[35] F. E. L. da Cruz, S. R. Lopes, and T. de Lima Prado, How to compute the minimum diagonal length of recurrence quantifiers to optimize their sensitivity to deterministic and stochastic properties, Chaos Solit. Fractals **173**, 113747 (2023).

[36] T. K. March, S. C. Chapman, and R. O. Dendy, Recurrence plot statistics and the effect of embedding, Phys. Lett. A **200**, 171 (2005).

[37] J. S. Iwanski and E. Bradley, Recurrence plots of experimental data: To embed or not to embed? Chaos **8**, 861 (1998).

[38] T. L. Prado, G. Corso, G. Z. dos Santos Lima, R. C. Budzinski, B. R. R. Boaretto, F. A. S. Ferrari, E. E. N. Macau, and S. R. Lopes, Maximum entropy principle in recurrence plot analysis on stochastic and chaotic systems, Chaos **30**, 043123 (2020).

[39] Y. Hirata and J. M. Amigó, A review of symbolic dynamics and symbolic reconstruction of dynamical systems, Chaos **33**, 052101 (2023).